



# Redetermination of the 450 °C isothermal section of the Al–P–Zn ternary phase diagram

Younian Zhu<sup>a,b,c</sup>, Jianhua Wang<sup>a,b,c</sup>, Xinming Wang<sup>b</sup>, Haoping Peng<sup>b</sup>, Xiaoqin Li<sup>b</sup>, Zhi Li<sup>b</sup>, Xuping Su<sup>a,b,c,\*</sup>

<sup>a</sup> School of Materials Science and Engineering, Changzhou University, 1 Gehu Road, Changzhou, Jiangsu 213164, PR China

<sup>b</sup> School of Mechanical Engineering, Xiangtan University, Xiangtan, Hunan 411105, PR China

<sup>c</sup> Key Laboratory of Advanced Metallic Materials of Changzhou City, Changzhou University, Changzhou, Jiangsu 213164, PR China

## ARTICLE INFO

### Article history:

Received 9 April 2011

Received in revised form

17 November 2011

Accepted 25 November 2011

Available online 6 December 2011

### Keywords:

AlP phase

Al–P–Zn ternary system

Phase equilibrium

## ABSTRACT

To obtain Zn-rich corner of the 450 °C isothermal section of the Zn–Fe–Al–P quaternary system, the 450 °C isothermal section of the Al–P–Zn ternary phase diagram was investigated experimentally again using scanning electron microscopy coupled with energy dispersive X-ray spectroscopy, and X-ray diffraction. The experimental results reveal that AlP is in equilibrium with L–Zn,  $\alpha$ -Al,  $Zn_3P_2$ , and  $ZnP_2$ , respectively. P solubility in liquid Zn and in  $\alpha$ -Al phases is limited. L–Zn +  $Zn_3P_2$  + AlP, L–Zn +  $\alpha$ -Al + AlP and  $Zn_3P_2$  +  $ZnP_2$  + AlP three-phase equilibria were well established in present work.

© 2011 Published by Elsevier B.V.

## 1. Introduction

In hot-dip galvanizing, both aluminum and phosphorus have great impacts on zinc alloy coatings. In general, small amounts of aluminum were added to zinc bath to control the reaction between Fe and Zn by forming an inhibition layer [1–3]. Phosphorus in steel was found to segregate in grain boundaries and limit the short-circuit diffusion of Zn atoms into  $\alpha$ -Fe [4], which could restrain the alloying reaction between Fe and Zn [5,6]. The phase equilibrium and thermodynamic information for the Zn–Fe–Al–P quaternary system are important to understand the combined effect of Al and P on the Fe–Zn reaction. Recently, Tu et al. [7] determined experimentally and assessed the Al–P–Zn ternary system at 450 °C. In the Zn-rich corner of this system, there exist a single phase region (liquid Zn) and a two-phase region (L–Zn +  $Zn_3P_2$ ). But in our recent work, it was found that in the Zn-rich corner of the 450 °C isothermal section of the Zn–Fe–Al–P quaternary system, the AlP phase exists in all the equilibrium alloys. On the basis of this fact, it is inferred that a two-phase region (L–Zn + AlP) should exist in the Zn-rich corner of 450 °C isothermal section of Al–P–Zn ternary system. However, the inferred phase equilibria in Zn-rich corner of

Al–P–Zn ternary system does not agree with that obtained by Tu et al. [7]. To obtain correct phase equilibrium in the Zn-rich corner of the 450 °C isothermal section of the Zn–Fe–Al–P quaternary system, the 450 °C isothermal section of the Al–P–Zn ternary phase diagram was investigated experimentally again.

## 2. Experimental methods

The Al–P–Zn isothermal section at 450 °C was determined again using equilibrated alloys approach. The design compositions of the alloys are listed in Table 1 (column 2). Composition points (A1–A8) are the same as those designed by Tu et al. [7]. The purity of all materials is 99.99%. Each sample, consisting of pure Zn, Al and P powders, was prepared by carefully weighing 3 g in total. All masses were weighed to an accuracy of 0.0001 g. Since aluminum would react with quartz tube at high temperature, the powders of the three elements were mixed and put into a corundum crucible which was sealed in an evacuated quartz tube. Each alloy mixture was heated to 1000 °C (which is much higher than the estimated liquidus temperature in Tu's experiment [7]) and kept at this temperature for 3 days, followed by quenching in water using a bottom-quenching technique [8] to minimize Zn loss and to reduce alloy porosity. The quenched samples were annealed at 450 °C for 60 days to ensure the establishment of equilibrium state. The treatment was completed with rapid water quenching to preserve the equilibrium state at 450 °C.

It has been reported that the AlP phase can react rapidly with water to form  $PH_3$  and aluminum hydroxide [9]. The reaction is as follows:



To prevent the occurrence of reaction (1), the preparation of the specimens consists of only two steps, including mounting and dry grinding. The conventional wet polishing was not used during the preparation of the specimens. The specimens were etched with an initial solution for revealing their microstructures. A JSM-6360LV scanning electron microscope (SEM) equipped with OXFORD INCA energy

\* Corresponding author at: School of Materials Science and Engineering, Changzhou University, 1 Gehu Road, Changzhou, Jiangsu 213164, PR China. Tel.: +86 5196338982; fax: +86 5196330095.

E-mail address: [sxping@cczu.edu.cn](mailto:sxping@cczu.edu.cn) (X. Su).

**Table 1**  
Compositions of alloys and phases in the Al–P–Zn system (at.%).

Alloy	Design composition	Phase	Zn	Al	P
A1	85Zn–5Al–10P	$\eta$ -Zn	99.5	0.3	0.2
		$Zn_3P_2$	56.9	0.8	42.3
		AIP	1.0	48.5	50.5
A2	80Zn–10Al–10P	$\eta$ -Zn	99.1	0.9	0
		AIP	1.4	48.5	50.1
A3	60Zn–35Al–5P	$\eta$ -Zn	72.9	27.1	0
		$\alpha$ -Al	39.2	60.5	0.1
		AIP	0.9	48.9	50.2
A4	40Zn–50Al–10P	$\eta$ -Zn	71.6	28.3	0.1
		$\alpha$ -Al	39.3	60.4	0.3
		AIP	1.2	48.7	50.1
A5	30Zn–50Al–20P	$\eta$ -Zn	74.7	25.2	0.1
		$\alpha$ -Al	39.4	60.4	0.2
		AIP	1.0	49.0	49.9
A6	30Zn–60Al–10P	$\alpha$ -Al	38.8	61.0	0.2
		AIP	0.7	48.9	50.4
A7	20Zn–60Al–20P	$\alpha$ -Al	37.4	62.2	0.4
		AIP	0.8	49.3	49.9
A8	8Zn–72Al–20P	$\alpha$ -Al	15.9	84.1	0
		AIP	0.4	48.8	50.8
A9	93Zn–3Al–4P	$\eta$ -Zn	99.3	0.4	0.3
		$Zn_3P_2$	57.0	0.2	42.8
		AIP	1.2	48.9	49.9
A10	93Zn–5Al–2P	$\eta$ -Zn	98.4	1.4	0.2
		AIP	1.3	49.5	49.2
A11	50Zn–5Al–45P	$Zn_3P_2$	56.8	0.1	43.1
		$ZnP_2$	32.1	0	67.9
		AIP	1.1	51.0	47.9

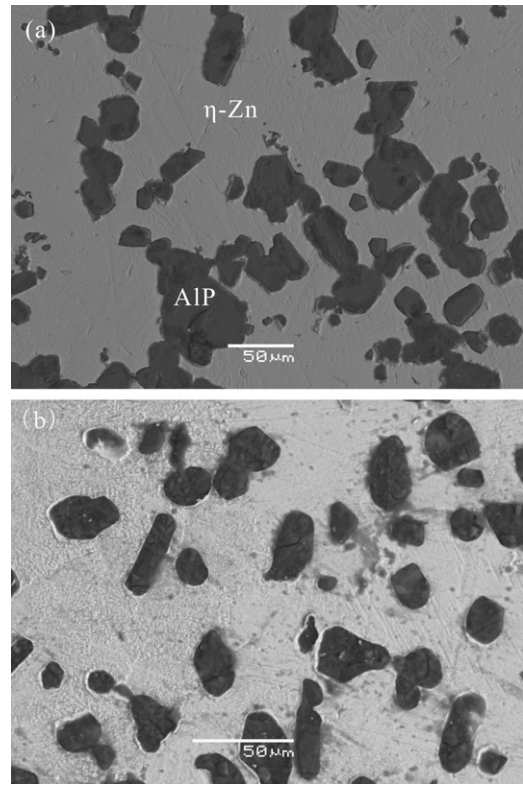


**Fig. 2.** The microstructure of alloy A2 shows the alloy consists of  $\eta$ -Zn and AIP phases. (a) Mounting and dry grinding was used. (b) The conventional way was used for the preparation of the specimen.

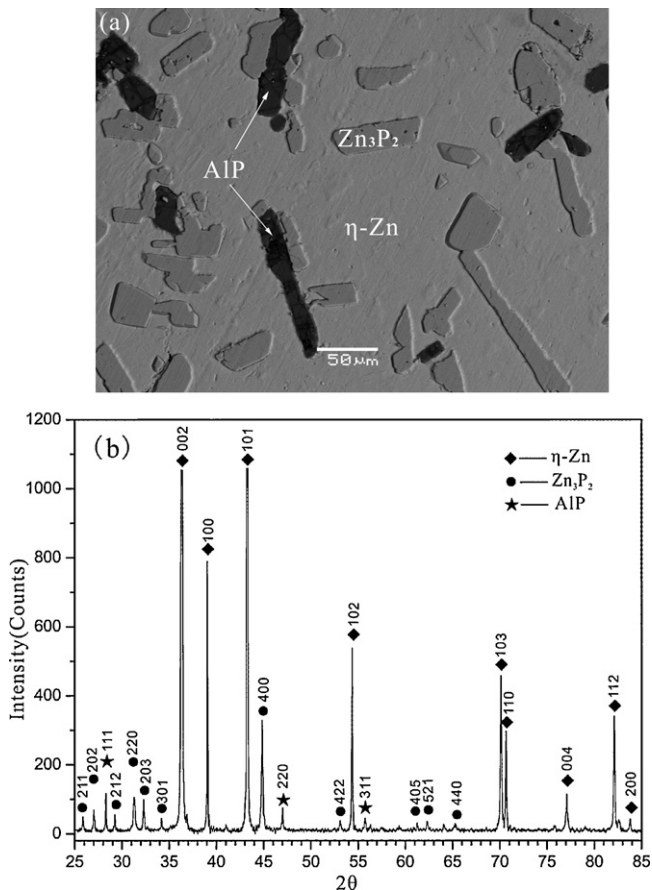


**Fig. 1.** The microstructure (a) and x-ray diffraction pattern (b) of alloy A1. The  $\eta$ -Zn,  $Zn_3P_2$ , and AIP phases coexist in a three-phase equilibrium state.

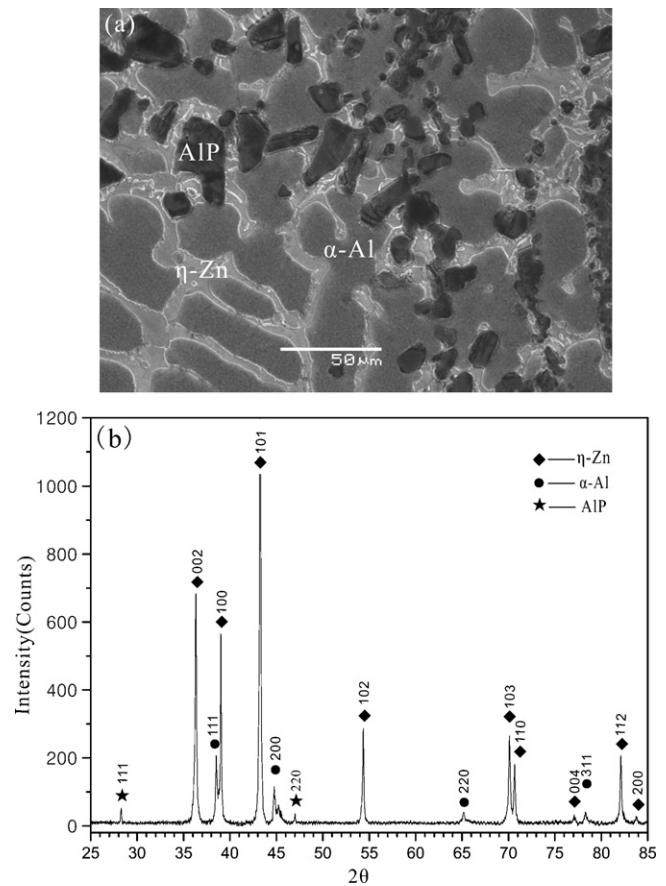


**Fig. 3.** The microstructure (a) and X-ray diffraction pattern (b) of alloy A3. The  $\eta$ -Zn,  $\alpha$ -Al, and AIP phases exist in a three-phase equilibrium state.

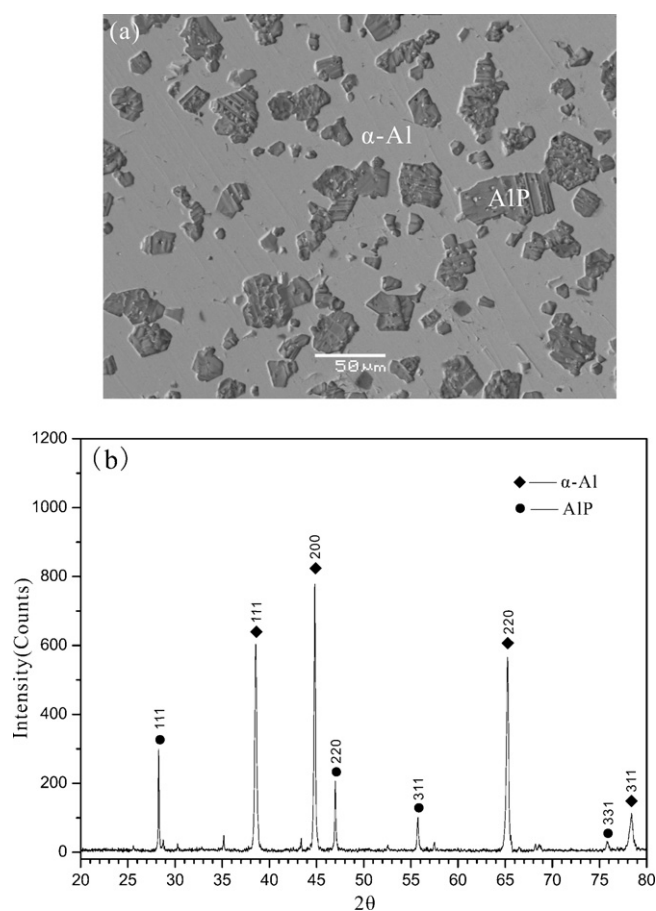


**Fig. 4.** The microstructure (a) and X-ray diffraction pattern (b) of alloy A8. The  $\alpha$ -Al and AIP phases exist in a two-phase equilibrium state.

dispersive X-ray spectroscopy (EDS) was used to study the morphology and chemical compositions of various phases of the alloys. The phase makeup of the alloys was further confirmed by analyzing X-ray diffraction patterns generated by a Bruker D8 advanced X-ray diffractometer, operating at 40 kV and 100 mA with Cu K $\alpha$  radiation.

### 3. Results and discussion

By means of the SEM-EDS technique, phases in alloys can be easily differentiated based on the relief, color and chemical compositions. The final identities of the phases were confirmed by analyzing the relevant X-ray diffraction patterns. All phases found in the alloys are listed in Table 1 (column 3) together with the chemical compositions (columns 4–6) determined by the SEM-EDS. The compositions are the averages of at least five measurements.

SEM-EDS analyses indicate that alloy A1 and A9 contain three phases:  $\eta$ -Zn,  $Zn_3P_2$  and AIP. During water quenching, the liquid Zn phase solidified and became the  $\eta$ -Zn phase. The microstructure and X-ray diffraction pattern of the alloy A1 are shown in Fig. 1. It can be seen that the  $Zn_3P_2$  and AIP phases uniformly distribute within the matrix of the  $\eta$ -Zn phase. The solubility of Al in the  $Zn_3P_2$  phase is less than 1 at.%.

Alloys A2 and A10 consist of the  $\eta$ -Zn and AIP phases. Fig. 2a shows the microstructure of alloy A2. EDS analyses reveal P solubility in the  $\eta$ -Zn phase is very limited. Using the conventional way for the preparation of the specimen, the AIP phase reacted with water, and the surface of the sample became very loose as shown in Fig. 2b. The original AIP phase changed into the other reaction products. The EDS results indicate that the average composition of the reaction products are O: 64.2 at.%, Al: 32.6 at.%, P: 2.7 at.% and Zn: 0.5 at.%.

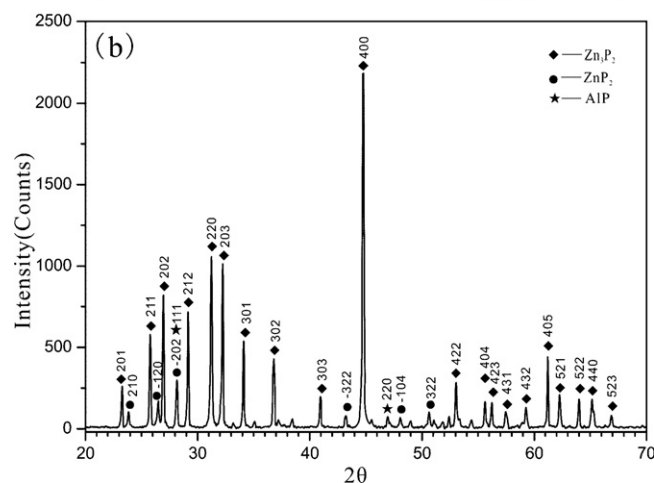
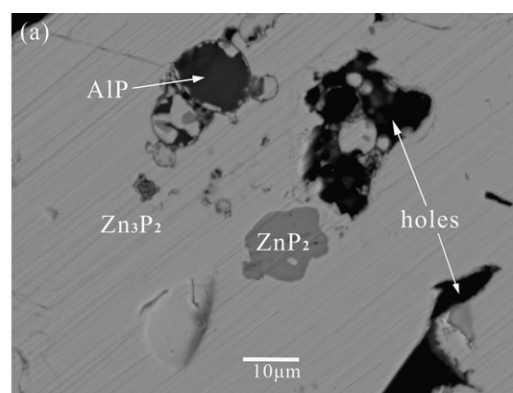


**Fig. 5.** The microstructure (a) and X-ray diffraction pattern (b) of alloy A11. The  $Zn_3P_2$ ,  $ZnP_2$ , and AIP phases exist in a three-phase equilibrium state.

The coexistence of  $\eta$ -Zn,  $\alpha$ -Al and AIP was found by the examination of the microstructures of alloys A3, A4 and A5. The microstructure of alloy A3 is shown in Fig. 3a. EDS analyses indicate that Zn solubilities in  $\alpha$ -Al and AIP phases are approximately 39 at.% and 1 at.%, respectively. The P solubility in  $\eta$ -Zn and  $\alpha$ -Al is limited. The XRD pattern of alloy A3 is shown in Fig. 3b which confirms the three-phase ( $\eta$ -Zn +  $\alpha$ -Al + AIP) equilibrium state of the alloy.

The microstructures of alloys A6, A7 and A8 indicate that the alloys consist of two phases: AIP and  $\alpha$ -Al. The microstructure and XRD pattern of the alloy A8 are shown in Fig. 4a and b. The Zn solubility in  $\alpha$ -Al phase decreases from 38.8 at.% to 15.9 at.% with the decrease of Zn in the alloy A6 to A8 from 30 at.% to 8 at.%.

Alloy A11 contains three phases:  $Zn_3P_2$ ,  $ZnP_2$ , and AIP phase, which is confirmed by its microstructure and X-ray diffraction pattern as shown in Fig. 5a and b. The sample is very brittle so as to powder easily during its preparation. Many holes exist in the specimen.

Tu et al. [7] did not find the existence of the AIP phase in alloy A1–A8. They only found that  $Zn_3P_2$  was in equilibrium with  $\alpha$ -Al in the Al–P–Zn system. The possible reasons for their observation may be as follows. The heating temperature for these alloys was not sufficient high in Tu's experiments considering the high vapor pressure of phosphorus and the low melting temperature of zinc, aluminum and phosphorus. At that temperature, zinc became liquid and aluminum was still in solidus state. Phosphorus would react with the liquid zinc easily, resulting in the formation of large amount of  $Zn_3P_2$  phase. This phenomenon could be confirmed by the following experimental results. The microstructure of alloy A1 quenched in water after being melted at 630 °C for two days, as shown in Fig. 6a, shows that only the  $Zn_3P_2$  and  $\eta$ -Zn phases coexist in the

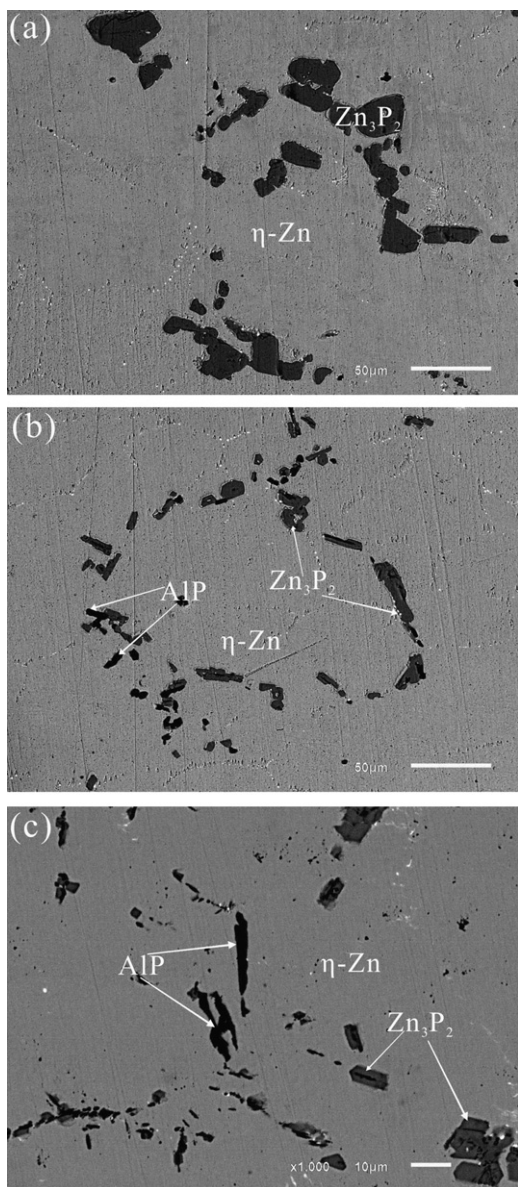


**Fig. 6.** The microstructure of alloy A1 (a) melted at 630 °C for 2 days (b) melted at 630 °C for 2 days and annealing at 450 °C for 21 days (c) melted at 750 °C for 2 days.

alloy. After diffusion annealing at 450 °C for 21 days, some AIP particles formed in the alloy as shown in Fig. 6b. When the alloy A1 was melted at 750 °C for two days, there exist still some blocks of  $Zn_3P_2$  phase in the alloy as shown in Fig. 6c. Alloy A4, which was melted at 630 °C for two days, consisted of small amount of  $\eta$ -Zn and a large amount of  $\alpha$ -Al and  $Zn_3P_2$  phases as shown in Fig. 7a. After diffusion annealing at 450 °C for 21 days, a lot of  $Zn_3P_2$  phase still existed in the alloy as shown in Fig. 7b. When the alloy A4 was melted at 750 °C for two days, the  $\eta$ -Zn,  $\alpha$ -Al, AIP and  $Zn_3P_2$  phases could be seen in the alloy as shown in Fig. 7c.

When the melting temperature of these alloys is below the melting point of aluminum, the reaction between zinc and phosphorus was very quick, but that between aluminum and phosphorus was much slow. So a lot of  $Zn_3P_2$  phase could be found, while the AIP phase could not be found in the alloy samples. It was difficult for Al–P–Zn system to reach equilibrium state only annealing at 450 °C for 21 days once the  $Zn_3P_2$  phase formed in these alloys.

It can be known from Al–P binary phase diagram [10] that the melting point of AIP is more than 2400 °C. The melting point of

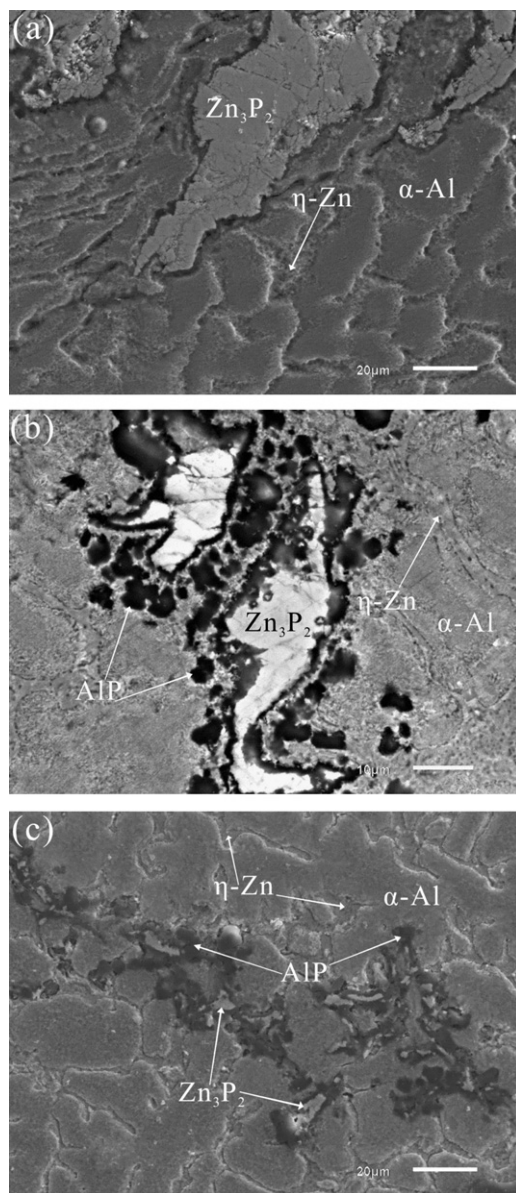


**Fig. 7.** The microstructure of alloy A4 (a) melted at 630 °C for 2 days (b) melted at 630 °C for 2 days and annealing at 450 °C for 21 days (c) melted at 750 °C for 2 days.

$Zn_3P_2$  phase is only 1173 °C as known in Zn–P binary phase diagram [11]. These two phases would exist stably at high temperature. In our experiments, the alloy samples were heated to 1000 °C for 3 days. The reaction between aluminum and phosphorus was very entirely at this temperature. The  $Zn_3P_2$  phase formed during the heating process disappeared after these alloy samples were kept at 1000 °C for 3 days. It was found that only the AIP phase could exist in those water quenched samples (A2–A8) indeed and the  $Zn_3P_2$  phase did not occur in these alloys.

Based on the results of microstructural studies and phase analyses, including SEM-EDS and XRD analyses, and by consulting the Al–P [10], P–Zn [11], and Al–Zn [12] systems, the 450 °C isothermal section of Al–P–Zn ternary system is proposed in Fig. 8.

#### 4. Conclusions

The 450 °C isothermal section of the Al–P–Zn ternary system has been investigated experimentally again in the present work. The new obtained results are summarized as follows:

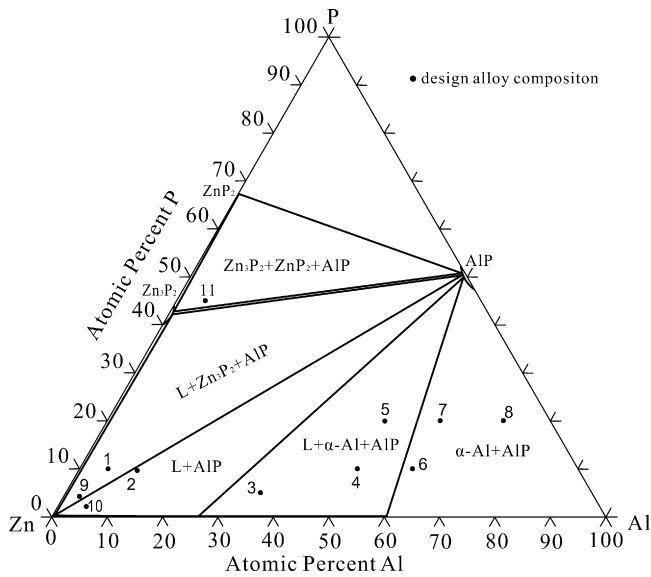


Fig. 8. The isothermal section of the Al–P–Zn ternary system at 450 °C.

1. The AIP compound was found to be in equilibrium with L–Zn,  $\alpha$ -Al,  $Zn_3P_2$  and  $ZnP_2$  phase respectively in 450 °C isothermal section of the Al–P–Zn ternary system.

2. P solubility in liquid Zn and in  $\alpha$ -Al phases is limited, and the AIP compound contains about 1 at.% Zn at 450 °C.
3. (L–Zn +  $Zn_3P_2$  + AIP), (L–Zn +  $\alpha$ -Al + AIP), and ( $Zn_3P_2$  +  $ZnP_2$  + AIP) three-phase regions exist in the 450 °C isothermal section of Al–P–Zn ternary system.

### Acknowledgments

This work is financial supported by the National Natural Science Foundation of China (Nos. 50971111 and 50971110) and sponsored by Qing Lan Project.

### References

- [1] M. Urednieck, J.S. Kiraldy, Z. Metallkd. 64 (1973) 899–910.
- [2] C.E. Jordan, A.R. Marder, J. Mater. Sci. 32 (1997) 5603–5610.
- [3] V. Furdanowicz, C.R. Shastry, Metall. Mater. Trans. A 30 (1999) 3031–3044.
- [4] L. Allegra, R.G. Hart, H.E. Townsend, Metall. Trans. A 14 (1983) 401–411.
- [5] C.S. Lin, M. Meshii, Metall. Mater. Trans. B 25 (1994) 721–730.
- [6] A. Nishimoto, J.I. Inagaki, K. Nakaoka, J. Iron Steel Inst. Jpn. 72 (1986) 989–996.
- [7] H. Tu, F. Yin, X. Su, Y. Liu, X. Wang, CALPHAD 33 (2009) 755–760.
- [8] X.P. Su, N.-Y. Tang, J.M. Toguri, Can. Metall. Q. 40 (2001) 377–384.
- [9] J.R. Wazer, Phosphorus and its Compounds, Interscience Publishers, Inc., New York, 1958.
- [10] A.J. McAlister, Bull. Alloy Phase Diag. 6 (1985) 222–224.
- [11] J. Dutkiewicz, J. Phase Equilib. 12 (1991) 435–438.
- [12] S.A. Mey, Z. Metallkd. 84 (1993) 451–455.